Estonian Journal of Earth Sciences, 2021, **70**, 3, 140–151 https://doi.org/10.3176/earth.2021.10

Geophysical mapping of residual pollution at the remediated Inčukalns acid tar lagoon, Latvia

Janis Karušs, Kristaps Lamsters, Dmitrijs Poršņovs, Viesturs Zandersons and Jurijs Ješkins

Faculty of Geography and Earth Sciences, University of Latvia, Jelgavas Street 1, Riga, LV-1004, Latvia; janis.karuss@lu.lv

Received 3 March 2021, accepted 15 April 2021, available online 20 June 2021

Abstract. Acid tar lagoons (ATLs) are a common environmental problem which is widespread in industrialized countries worldwide. Such lagoons have become significant and massive sources of environmental pollution affecting the soil, atmosphere and surface and ground waters. In this study, we characterize the distribution of the residual soil and groundwater pollution plume in the vicinity of the southern Inčukalns ATL (Latvia), using coupled ground-penetrating radar (GPR) and electrical resistivity tomography (ERT) data. The obtained geophysical data provide information about the geological structure and the distribution of the acid tar contamination plume. We determined the location of the low-resistivity zone and related it to the distribution of the contamination. Our study demonstrates that the applied combination of GPR and ERT is an effective tool for analysing the geospatial distribution of ground and groundwater pollution plumes caused by ATLs in areas with complex geological cross-sections.

Key words: ground-penetrating radar, electrical resistivity tomography, groundwater and soil pollution, acid tars, toxic waste.

INTRODUCTION

Acid tars (ATs) are a hazardous and persistent pollutant. They are the result of industrial chemical waste from the treatment processes of organic materials using concentrated sulphuric acid (oleum) to remove unwanted impurities (e.g. sulphur-containing compounds and/or unsaturated hydrocarbons). Large amounts of this substance have been formed in the past through the processes of refining benzol, used lubricating oils and the production of white mineral oils (Milne et al. 1986). The consistency of ATs is highly resinous and viscous (Kolmakov et al. 2006). The state and flowability of this material depend largely on temperature: it is fluid at higher temperatures but becomes solid when the temperature drops. The flowability of ATs is also altered by weathering processes: a layer of permanently solid weathered substance can usually form on the surface of AT if it is exposed to the weather. The density of ATs (1200–1400 kg/m^3) is much higher than of other types of tar due to the presence of sulphuric acid. The properties of ATs are similar to those of Dense Non-Aqueous Phase Liquids (DNAPLs). However, AT cannot be classified as a DNAPL due to its partial solubility in water (Hao 2007). The composition of ATs is complex and variable, depending on the sample's origin (Milne et al. 1986). It is dependent not only on the process from which it originates, but significant differences may also be found even between every two batches of ATs coming from the same factory (Nancarrow et al. 2001; Hao 2007). Analyses of two AT samples originating from the petroleum industry (Leonard et al. 2010) have demonstrated that this substance consists of a wide range of aliphatic and cyclic organic compounds, including polycyclic aromatic hydrocarbons (PAHs), pyrroles, phthalates, thiophenes and organic acids (e.g. carboxylic, sulphonic) together with massive amounts of free sulphuric acid. The ash of AT originating from petroleum processing or spent lubricant re-refining is rich in manganese, cadmium and metalloids (Leonard et al. 2010). The dangerous properties of ATs include their extreme acidity (pH = 1–2), corrosiveness and multiple types of toxicity (Milne et al. 1986; Leonard et al. 2010). Many of AT toxic compounds, such as aliphatic organics, PAHs and heavy metals, express significant mobility and are easily leachable (Leonard et al. 2010).

Acid tars were produced in large quantities between the end of the 19th century and the 1980s until alternatives for sulphuric acid treatment were found. The sustainable utilization methods were unknown at that time (Milne et al. 1986). Thus the dumping of ATs in sand and gravel quarries or other pre-existing pits in the ground was a standard method for managing this type of waste. Such a manage-

ment method led to the formation of acid tar lagoons (ATLs), which are a common environmental problem that is widespread in industrialized countries worldwide. Scientific reports on the problem of ATLs, for example, in Germany (Gruss 2005), Belgium (Pensaert 2005), USA (Grajczak & McManus 1995), Russia (Kolmakov et al. 2006), Slovenia (Družina & Perc 2010), France (Naudet et al. 2011, 2014) and the UK (Reynolds 2002; Hao 2007) can be found in the literature, while the extent of the problem has not been limited to these countries.

Organic compounds are leached from ATLs in the form of solutions and insoluble organic colloids. In contrast, inorganic compounds migrate mostly in the form of a water solution (Hao 2007). Acid tar lagoons are also a source of atmospheric pollution with sulphur dioxide, especially being released during the handling and soon after disposal (Pensaert 2005). The weathering of ATs can also result in the development of other gaseous pollutants, e.g. hydrogen sulphide and methane (Nancarrow et al. 2001). Therefore, ATLs usually become significant and massive environmental pollution sources affecting the soil, atmosphere and surface and ground waters.

Studies of ATLs and the ground pollution around them are ambiguous due to the highly toxic nature of such lagoons. Traditional investigation methods include drillings and sampling; however, such an approach has significant shortcomings. The obtained data provide information only at selected locations, and drilling a well can create new paths for the migration of the pollutant (Reynolds 2002; Naudet et al. 2011). Elevated levels of acidity and corrosiveness also put workers under serious health risks during the installation of wells. An alternative approach includes the application of geophysical methods that have been proven to provide valuable information not only in many cases of DNAPL contamination investigations (Jiang et al. 2013; Power et al. 2015) but also specifically in ATL investigations (Chambers et al. 1999; Reynolds 2002; Naudet et al. 2011, 2014).

This study aims to characterize the distribution of the residual soil and groundwater pollution plume in the vicinity of the southern Inčukalns ATL (Latvia) at the end of an environmental clean-up project of the lagoon via the coupled ground-penetrating radar (GPR) and electrical resistivity tomography (ERT) data. Such a complex geophysical approach complemented by the existing monitoring well data serves to develop and improve methodologies for investigating pollution caused by ATLs. It also provides environmental geologists with a powerful and cost-effective problem-solving tool that can be used in highly problematic pollution hotspots all over the world.

STUDY AREA

The Inčukalns ATLs were located in two old sand quarries near the village of Inčukalns ~30 km NE of Riga, Latvia (Fig. 1). Both northern and southern lagoons were made

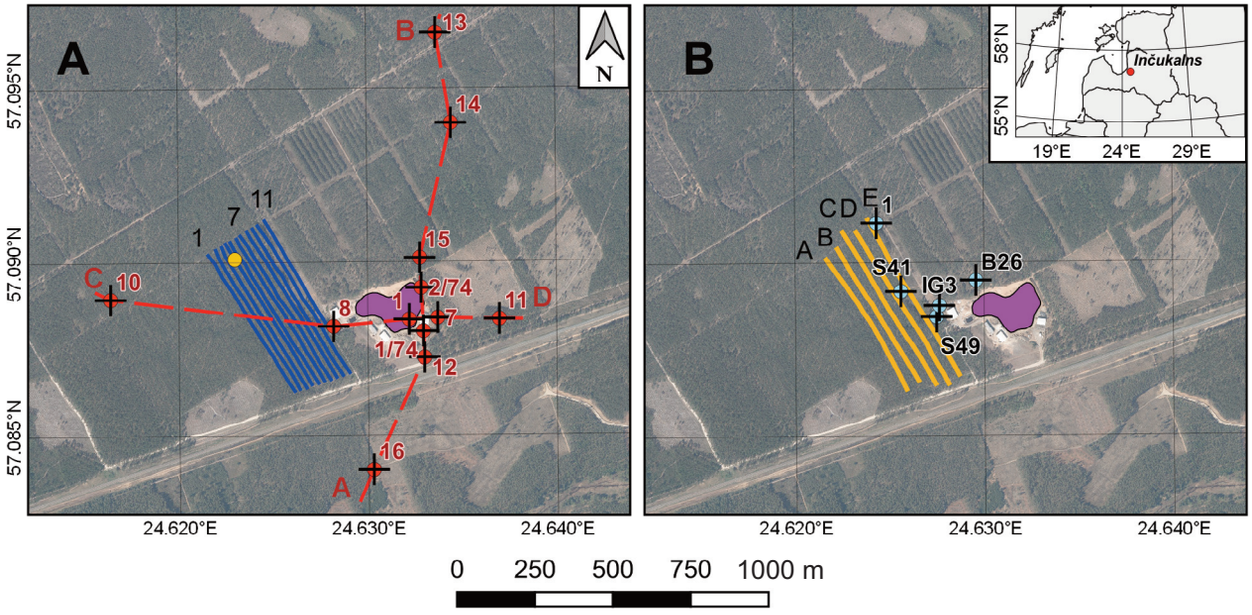

Fig. 1. Overview of the survey area. **A**, location of the ground-penetrating radar profile lines (blue). The red dashed line marks lines of the geological cross-section. The yellow dot marks the point where common midpoint measurements were done. Black crosses mark the locations of boreholes. The purple polygon marks the acid tar lake. **B**, location of the electrical resistivity tomography profile lines (yellow). Black crosses mark the locations of groundwater monitoring wells. The purple polygon marks the acid tar lake.

in sandy soil without effective isolation measures either at the bottom or on the sides (Karuša & Demidko 2018).

Our study site was situated next to the southern ATL. The geological setting of that site is rather complicated because of the discontinuous layer of glacial till (Fig. 2). Additionally, a hydrological connection exists between Quaternary and Devonian aquifers, providing the passage of pollution (Aleksans et al. 1993, 1994). The Middle Devonian bedrock lies at 15–25 m a.s.l. and consists mainly of sandstone with interlayers of claystone and siltstone of the Gauja Regional Stage. The interlayers can be considered as partial aquitards for the groundwater. The lower part of the Gauja Stage is well isolated from the upper part by up to 28-m-thick claystone. The bedrock is covered by clayey and sandy glacial till of the Weichselian glaciation with a thickness reaching 6 m. However, commonly it is only a few metres thick and utterly absent in places (Berzina & Samushenkov 1977). Such a situation occurs, for example, directly beneath the southern ATL and across our study site, where sandy sediments directly

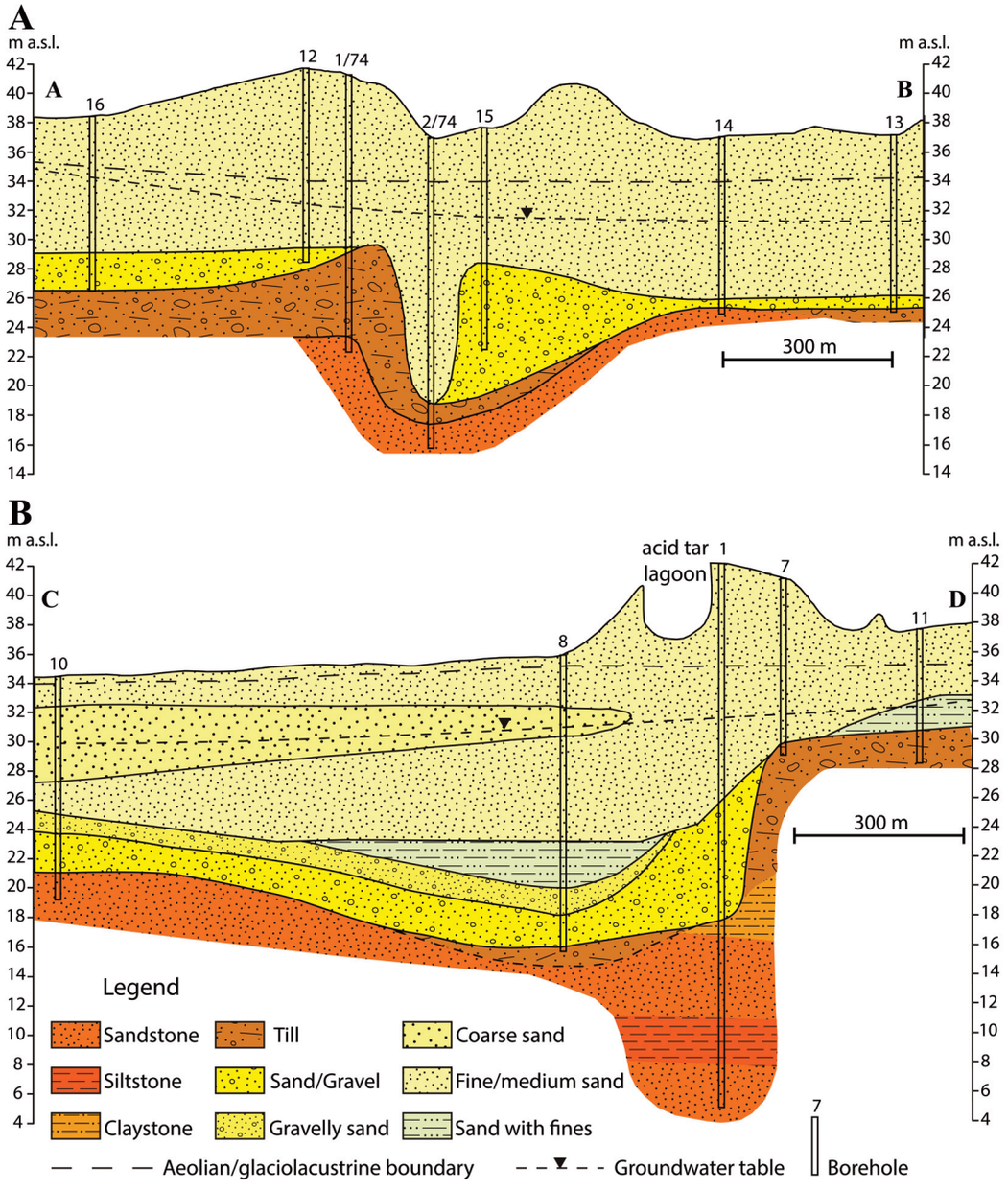

Fig. 2. Geological cross-section of the study area (after Berzina & Samushenkov 1977). **A**, cross-section A–B; **B**, cross-section C–D. For location see Fig. 1.

overlie the bedrock. The overall permeability of glacial till is minimal and limited to only 0.0004 m/day (Karuša & Demidko 2018).

Most of the Quaternary sediments comprise glaciolacustrine sands of the Zemgale ice-dammed lake that overlies gravelly sands and a mixture of sands and gravel. These sandy/gravelly sediments are characterized by a high permeability reaching the highest value of 38 m/day near the southern ATL (Karuša & Demidko 2018). The upper part of the Quaternary sedimentary sequence consists of aeolian sediments with variable thicknesses reaching more than 5 m in the highest inland dunes. The overall thickness of the Quaternary deposits in the study area near the southern ATL varies from 13 to 22 m, according to borehole data (Berzina & Samushenkov 1977).

Hydrogeological conditions can be described as well-suited for the infiltration of pollutants because of the absence of aquitards in places, both in Quaternary sediments and Devonian bedrock. The discontinuous distribution of the glacial till layer can be considered the main factor facilitating the infiltration of groundwaters into the artesian aquifers through so-called hydrological windows (Karuša & Demidko 2018). The groundwater table lies at 5–8 m from the ground surface, being deeper beneath dunes. The direction of overall groundwater flow in the study area is to the NW, although it is locally variable and depends on the variations in the altitude of the ground surface (Ņelajevs 2019). For example, groundwater tends to flow in the direction of artificial depressions located approximately in the middle of the study area (Fig. 1). According to the monitoring data of chemical pollutants, the area of geophysical mapping is located exactly at the site where maximal values of pollutants were identified in monitoring wells (Ņelajevs 2019).

The ATs in the Inčukalns ATL originated from the production of white oils in the petrochemical factories of Riga. Around 16 000 tonnes of ATs were dumped there every year between 1950 and 1980. The northern lagoon that is not studied here was used from the 1950s to 1970. The southern lagoon, investigated in this study, was in use from 1956 to 1981 (Kruglik 1990; Aleksans et al. 1993, 1994; Karuša & Demidko 2018). At the beginning of the 21st century, the area of the southern pond was ~1.3 ha under low precipitation conditions and ~1.6 ha at high precipitation, and it contained around 64 000 m^3 of ATs. The depth of the southern lagoon was ~3 m in the eastern part and ~4.5 m in the western part (Karuša & Demidko 2018). The Inčukalns ATL composition, reported by Berzina & Samushenkov (1977), comprises 5–60% tars and asphaltenes, 10–40% sulphonic acids, 35–50% sulphuric acid and less than 1% oils.

The first attempts to reduce the environmental pollution caused by the lagoons were made in 1988. These measures included the injection of 38 000 m^3 of tar mixed with 87 000 m^3 of polluted waters from the aquifers of the Amata–Aruküla (Arukila in Latvian) formations into the lowest, closed Cambrian structures up to depths of 800–900 m. However, the knowledge of these geological structures and movement of artesian waters was somewhat limited (Kruglik 1990; Aleksans 1993, 1994). A further 60 000 m^3 of AT diluted with polluted waters from Devonian aquifers were further injected in 1990 and 1991, reducing the size of the southern ATL by up to 20% (Kruglik 1990; Aleksans 1993, 1994). Remediation of analysed objects during the post-Soviet period faced severe problems typical for post-socialist countries: it was impossible to apply the 'polluter pay' principle. Changes in the economic system have led to the complete disappearance of historical factories. Therefore, Latvia was forced to use public funding from the EU's European Regional Development Fund to perform the remediation. Remediation took place in the area of the southern pond in 2007–2021. These activities included the excavation and neutralization of the tar mass using lime, mixing the neutralized mass with wood shavings and transporting the product to the cement plant for incineration (State Environmental Agency 2020).

MATERIAL AND METHODS

Geological data

Information about the general geological structure and the distribution of the pollution at the studied site was obtained using historical data and reports (e.g. Berzina & Samushenkov 1977; Kruglik 1990; Aleksans 1993, 1994) as well as currently used groundwater monitoring wells (see Fig. 1B). Currently, 19 monitoring wells exposing groundwater are installed at the Inčukalns site (Ņelajevs 2019). The exact location of the survey polygon was selected by analysing the information about the distribution of the pollution from monitoring wells. The selected area includes the site where the most severe groundwater pollution has been detected (Ņelajevs 2019).

Ground-penetrating radar survey

In this study, we used GPR Zond 12-e with 300 MHz and 75 MHz antennae. With the 300 MHz antenna, high-resolution data were obtained for the upper part of the survey area, while the 75 MHz antenna was used to determine the depth to the glacial till and/or bedrock. During the survey, using the 300 MHz antenna, the recording time was set to 500 ns (in sandy sediments, it corresponds to an approximately 25 m depth). The recording time was set to 800 ns when the 75 MHz

antenna was used (in sandy sediments, it corresponds to an approximately 40 m depth). Profiles were recorded with a regular spacing of 20 m between them. In total, 11 GPR profiles were recorded with a total length of more than 5.5 km, covering an area of 12 ha (Fig. 1A). To determine the exact location of the GPR profiles, an RTK GNSS receiver Emlid Reach RS2 was used. The exact coordinates of the profiles were measured every 50 m along the surveyed profiles. The LKS92/Latvia TM coordinate reference system was used for georeferencing purposes.

All the obtained radar records were processed in the *Prism 2.60* software. During processing, (1) time-dependent gain, (2) *Background removal* and (3) *Ormsby bandpass* filters were used to suppress signals that were not related to geological structures in the survey area.

To determine the GPR signal propagation speed, a common midpoint method (CMP) was applied (Neal 2004; Karušs & Bērziņš 2015), using a 300 MHz antenna as a transmitter and a 500 MHz antenna as a receiver. Both antennae were moved apart with respect to a central fixed position in a direction parallel to the common offset profile. The distance between separate traces was set to 0.1 m, while the final distance between transmitting and receiving antennae was approximately 9 m. The exact positions for the CMP measurement point were chosen using common offset radar records. The location where the deepest reflection (initially interpreted as the glacial till top surface) was visible was selected. For each radar record, relevant coordinates were added, and, by using the function *Annotation*, the depth of the deepest reflection along the surveyed profile was determined. Afterwards, the information about the deepest reflection depth was exported from *Prism 2.6* to *.txt files that were processed with *ArcMap 10.6*. Then, using ordinary kriging interpolation, a map of the glacial till/bedrock surface depth was produced.

Electrical resistivity tomography survey

An ERT survey was carried out using a multichannel *Syscal Pro Switch* (*IRIS Instruments*) device. Measurements were performed with 72 stainless steel electrodes and using the Wenner electrode configuration (Reynolds 1997). Spacings between electrodes were set to 2 m. Altogether five profile lines longer than 500 m (Fig. 1B) were recorded using a roll-along technique to save time (GeoTomo software 2017). All five profile lines consisted of five or six separate ERT profiles. The overlap of individual profiles was chosen to obtain continuous data coverage up to depths of approximately 12 m. The location of the ERT profiles was determined with an RTK GNSS receiver Emlid Reach RS2. The exact coordinates of the profiles were measured every 36 m along surveyed profile lines. Topography changes along the ERT and GPR profiles were determined using ground surface elevation from a LiDAR-derived digital elevation model.

The ERT data were processed using the RES2DINV software (*GeoTomo Software*). The first step of data processing was to manually check for any outliers. The signal that corresponded to the resistivity values of the ground changed gradually; therefore, any data points that noticeably differed from the surrounding points were likely to indicate problems with electrode contact with the ground during the measurements (Loke 2004). No more than a few outliers were found on each of the five profile lines. Least-squares inversions of apparent resistivity data were carried out using the quasi-Newton method (Loke & Barker 1996).

For the inversion process, the finite-element mesh was used. To obtain smoother results, the model refinement option, which uses model cells with widths of half the electrode spacing, was applied. The depth of the deepest prominent reflection determined by GPR was added to the dataset as a sharp boundary. No restriction of resistivity below this boundary was set during the inversion process. During the inversion process, the L_2 norm (Loke 2004) was applied and the effects of side blocks were reduced severely. The resulting models were topographically corrected to account for elevation changes along the profile lines and visualized using logarithmic contour intervals.

In this study, the geochemical analyses published by LTD Azurīts were used to correlate ground contamination. An inverse distance weighted interpolation method was used in *ArcMap 10.6.* to generate maps of the distribution of pollutants. Anionic surfactants and chemical oxygen demand were determined in the ALS laboratory (Czech Republic), sulphate ions were determined by the SIA 'AND resources' company (Riga, Latvia), while the Azurīts company performed groundwater sampling. All analyses and sampling procedures were conducted following the corresponding ISO standards (Ņelajevs 2019).

RESULTS AND DISCUSSION

Ground-penetrating radar survey

The geophysical data obtained in the selected study area provide information about the geological composition and distribution of AT contamination plumes. Numerous prominent reflections are visible in the obtained radar records (Fig. 3). From the CMP measurements it was determined that the dielectric permittivity down to the deepest reflection (reflection 1 in Fig. 3) was 13.7, while the dielectric permittivity down to the shallowest most

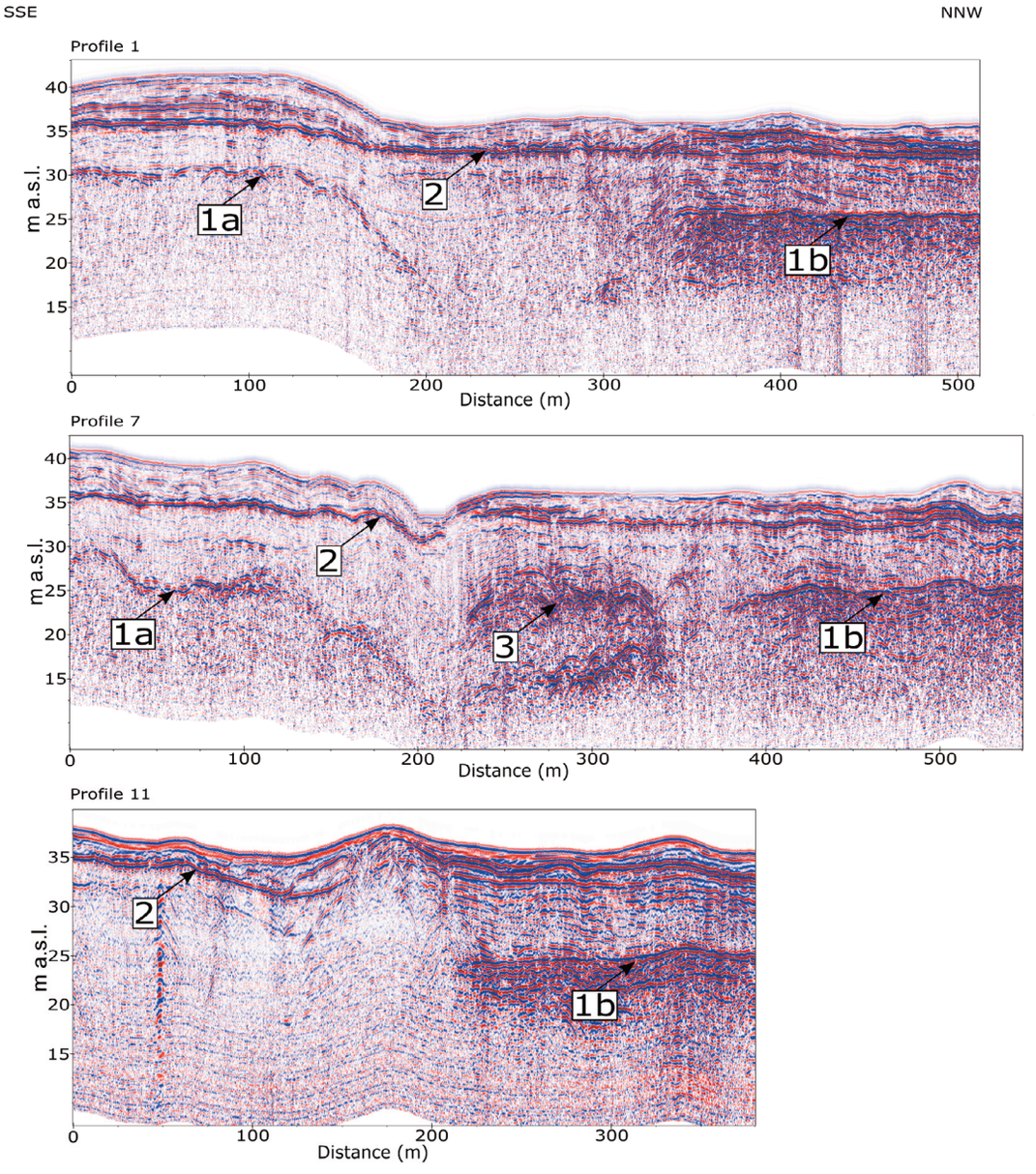

Fig. 3. Radar records obtained by using a 75 MHz antenna. 1a and 1b, reflections related to the base of sandy sediments; 2, reflection associated with the bottom of aeolian deposits; 3, reflections from a local zone of high dielectric contrast. For the location of the profiles, see Fig. 1A.

prominent reflection (reflection 2 in Fig. 3) was 5.9. The obtained values indicate relatively dry sandy sediments in the upper part of the geological cross-section, while saturated sandy sediments are most likely present between reflections 2 and 1 (Neal 2004).

The geological cross-section information down to a depth of 22 m was obtained considering the determined dielectric permittivity values from the data recorded with the 75 MHz antenna. In the radar records obtained with the 300 MHz antenna, only the shallowest parts or reflection 1 were evident.

We chose to divide reflection 1 into two parts (reflections 1a and 1b) as the sediments below this boundary showed significant differences along the surveyed profiles. We interpret reflections 1a and 1b as the base of the sandy and gravelly sediments (Fig. 3). The depth of the obtained reflections closely correlates with the depth of this boundary in boreholes (Karuša & Demidko 2018; Ņelajevs 2019; Figs 2, 3). On the southern side of the study area, reflection 1 was rather sharp, and no reflections below it were evident. This indicates the presence of sediments with high dielectric loss below this boundary

(Fig. 3, reflection 1a). On the northern side of the study area, reflection 1 was prominent as well. Still, there were also numerous clear reflections below this boundary, suggesting an environment with more minor dielectric losses (Fig. 3, reflection 1b). Our interpretation is that reflection 1a is related to the upper surface of glacial till, which is embedded below the sandy sediments. Such clayey glacial till usually prohibits the propagation of electromagnetic waves (Neal 2004; Lamsters et al. 2020). On the contrary, reflection 1b could be related to the surface of clastic bedrock (sandstones), which lies directly beneath the upper sandy, gravelly sediments, and the possible glacial till layer could be relatively thin or missing entirely. This interpretation fits well with the data obtained from boreholes (Berzina & Samushenkov 1977), revealing that a glacial till layer is absent and the bedrock is overlain directly by sandy, gravelly sediments in some parts of the survey area (Fig. 2).

Thus, our observations support the assumption that a possible connection exists between Quaternary and Devonian aquifers in the vicinity of the southern ATL hydrogeological window due to the lack of the glacial till layer (Berzina & Samushenkov 1977; Kruglik 1990; Aleksans 1993, 1994; Karuša & Demidko 2018; Ņelajevs 2019). The connection provides a direct migration path for the contamination.

A distinctive reflection from a depth of ~5 m was received (Fig. 3, reflection 2) across the whole of the survey area. The data obtained from boreholes (Berzina & Samushenkov 1977) indicate that a boundary between aeolian and glaciolacustrine sediments is embedded at this depth (Fig. 2). An alternative origin for this reflection could be related to the groundwater level that is also close to this depth. However, reflection 2 has pronounced undulations across all recorded profiles with steep variations in depth (Fig. 3, profiles 7, 11). As these changes were somewhat too erratic for the usually even groundwater table, we tended to link this reflection with the base of the aeolian deposits. These deposits are found across the study area and frequently compose inland dunes. Groundwater level was probably related to one of many weaker sub-horizontal reflections that can be seen on the obtained radar records (Fig. 3).

A zone of strong reflections was detected on several radar records in the middle part of the sandy sediment layer (reflection 3 in profile 7, see Fig. 3). Those reflections could be related to local changes in the granulometric composition and bedding of sediments, but it is hard to interpret them unambiguously without further borehole data.

Besides the reflections related to geological structures in the survey area, a zone with increased GPR signal losses was identified in the sandy sediments. For example, a clearly identifiable reflection (Fig. 3, 1b in profile 11) was abruptly lost in the southern part of the radar record. A similar situation was also evident in some of the other profiles not illustrated in this paper. Even in profile 7 there was a local decrease in the amplitude of reflection 1b at 380 m (Fig. 3). We relate such an abrupt increase in signal losses to increased electrical conductivity of groundwater in this particular zone. As determined from the following ERT results (Fig. 4) and the distribution of pollution in monitoring wells (Fig. 5), this zone of increased electrical conductivity could be interpreted as a zone highly contaminated by ATs.

Electrical resistivity tomography survey

Similar to GPR data, ERT data provided an insight into the geological structures and possible contamination of the study area. The upper parts of all the ERT profiles (Fig. 4) consist of a high-resistivity zone, which we interpret as sandy sediments considering the presence of typically high-resistivity aeolian and glaciolacustrine sand in the upper part of the geological cross-section (Fig. 2). An exception was a small area around the 224 m horizontal distance mark in profile D, related to an artificial depression in the ground with a locally higher groundwater table (Fig. 4, profile D).

In all the ERT profiles obtained, inverse modelling results revealed a low-resistivity layer below a sharp boundary incorporated in the model using the GPR data (Fig. 4). The ERT data support the interpretation that the observed sharp boundary in the southern part of the survey area coincides with the surface of the glacial till layer, as glacial till is usually characterized by low-resistivity values (Reynolds 1997). The same resistivity values represented the northern part of the ERT profiles where sandstone embeds directly below the sandy sediments, as evident from GPR and borehole data (Figs 2, 3). According to the interpretation of GPR and borehole data, we relate these low-resistivity values to the water-saturated sandstone (Reynolds 1997). The possible existence of a hydrological window (the connection between Quaternary and Devonian aquifers) that developed due to the lack of the glacial till layer could not be verified from the ERT data only.

In profiles A and B, a local zone of higher resistivity was observed at 470 m below the surface of glacial till and/or bedrock (Fig. 4). We explain this anomaly with the proximity to the model boundary that could create some artefacts in the model (Loke 2004). We discard the possibility that this anomaly is related to any geological structure or contamination. Similarly, there are some local vertical structures of high resistivity below the sharp boundary (Fig. 4, profiles C, D, E) that are most likely artefacts of the inversion process as the data coverage in the lower part of the model is not uniform and some areas lack sufficient coverage (Loke 2004).

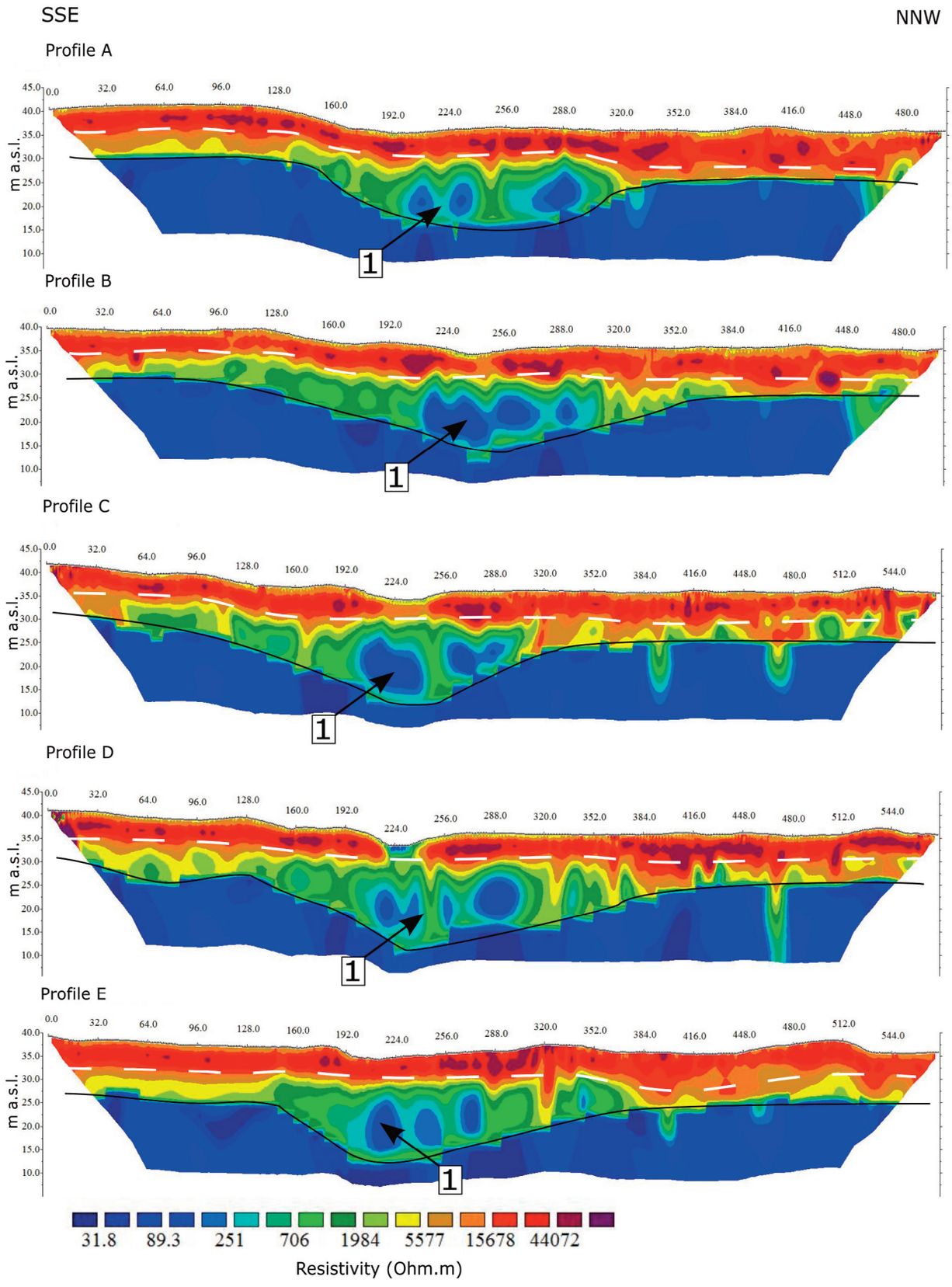

Fig. 4. Electrical resistivity tomography results. 1, a zone of low resistivity. The groundwater level is shown by the white dashed line. The black line represents the top of the low-resistivity layer. For the location of the profiles, see Fig. 1B.

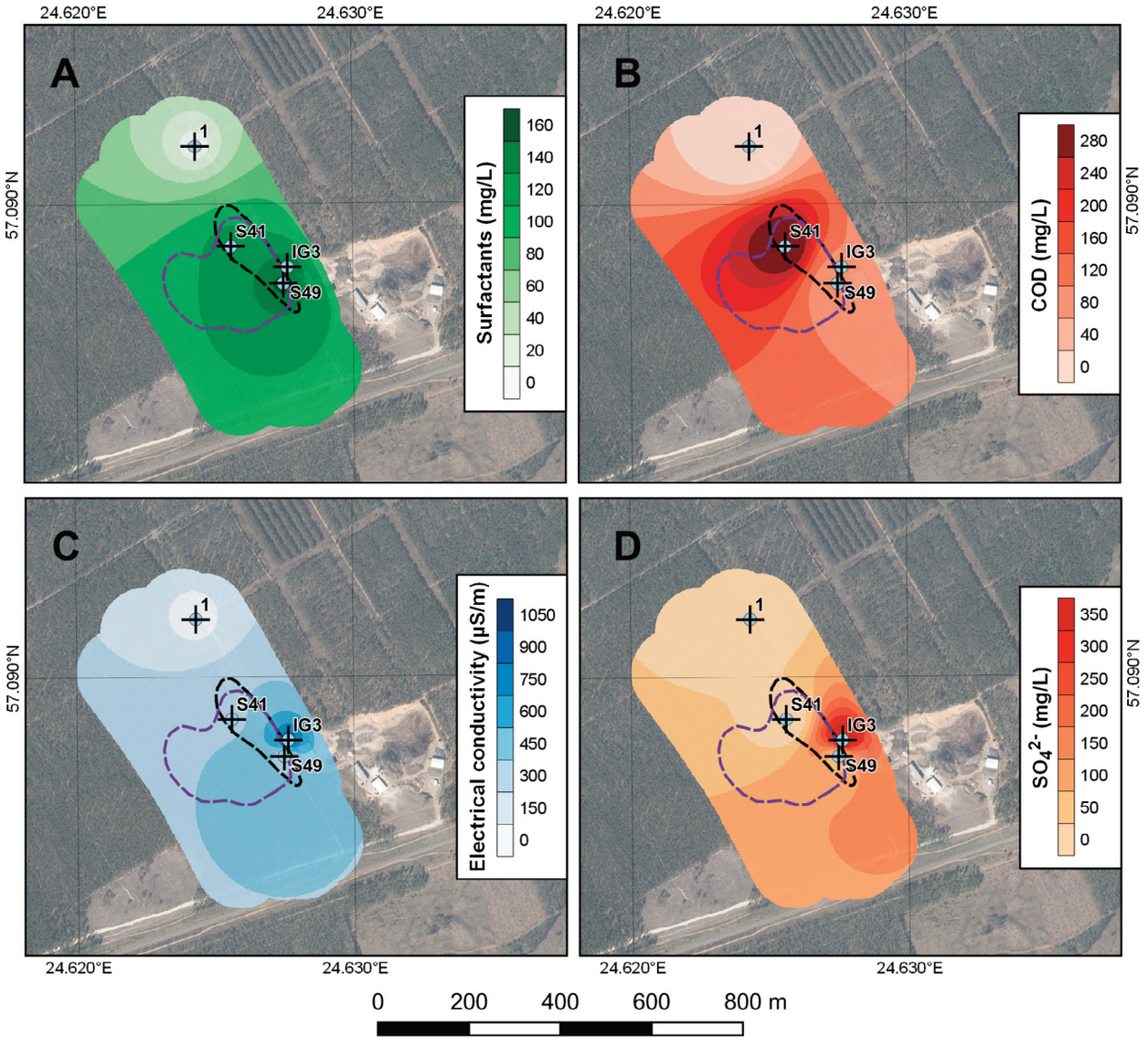

Fig. 5. Groundwater pollution that was determined at the boreholes (Nelajevs 2019). **A**, concentration of surfactants in groundwater; **B**, chemical oxygen demand in groundwater; **C**, electrical conductivity of groundwater; **D**, concentration of SO_4^{2-} in groundwater. The black dashed line represents the high-conductivity zone determined by ground-penetrating radar. The purple dashed line represents the high-conductivity zone determined by electrical resistivity tomography.

A rather sharp decrease in resistivity was observed in all ERT profiles at an approximate depth of 5 m (Fig. 4). We relate this increase to the groundwater level because the groundwater level was found at a similar depth in boreholes. Some minor and major variations in the resistivity values occurred below the groundwater level as well. The most prominent one was observed in the middle part of all the ERT profiles where a zone of low resistivity was present (see the black arrow in Fig. 4). We interpret this low-resistivity zone as a possible AT contamination plume which will be discussed further.

Distribution of the acid tar (AT) contamination

The low-resistivity zone revealed by ERT data (Fig. 4) coincides with a local depression in the glacial till surface (Fig. 4). The low-resistivity zone is situated below groundwater surface, suggesting that pollution is denser than groundwater. According to modern concepts that have been confirmed by experiments (Hao 2007), a gravity-driven downward migration characteristic of DNAPLs is the most essential mechanism in the distribution of ATs in geological environments as well.

The downward spreading of the free phase of AT occurs until the nonporous geological layer is reached and the lateral spreading of AT begins (Naudet et al. 2011, 2014). The downward spreading of AT explains why our observations suggest that a contamination plume possibly follows the local deepening rather than the regional direction of the groundwater flow to the north (Ņelajevs 2019).

Jiang et al. (2013) reported that DNAPL contamination created a high-resistivity area in ERT data which could seem contrary to our ERT data suggesting contamination that coincides with a low-resistivity zone. Although ATs have been classified as DNAPLs by some authors (Naudet et al. 2011, 2014), this point of view is incorrect. In contrast with typical DNAPLs, e.g. chlorine-organics that are completely insoluble in water, the presence of soluble free sulphuric acid and surface active sulphonic acids in ATs makes the interactions of this substance with water much more complex (Hao 2007). After the groundwater level is surpassed, the behaviour of AT becomes strongly different from that of a DNAPL: ATs mix and partially dissolve in water, forming complexes, colloidal, multiphase pollution plumes (Smith et al. 2008) with an improved migration ability under saturated conditions in comparison with the initial tars (Hao 2007).

The soluble part of AT is characterized by low resistivity (Chambers et al.1999; Naudet et al. 2014). Thus we relate the low-resistivity zone in our ERT data to the distribution of the contamination in groundwater. Similar results have been obtained in studies by Naudet et al. (2011) and Chambers et al. (1999), who both showed that leachates from ATLs were characterized as having low-resistivity (below 20 Ohm.m.) values. The results of Naudet et al. (2014) demonstrated a strong correlation between electrical resistivity measured by ERT and the concentration of pollutants in groundwater. In this study, we saw a similar pattern. In the area where the low-resistivity anomaly is present (Fig. 4), the greatest pollution concentration was also observed in boreholes (Fig. 5). We also observed a high-conductivity zone in GPR data that closely correlates with the measured distribution of groundwater contamination in the study area (Fig. 5). However, this high-conductivity zone interpreted from GPR data is smaller than the high-conductivity (or low-resistivity) zone interpreted from ERT data. The zone obtained from ERT data spreads further away from the ATLs and boreholes, where the greatest concentration of pollution was determined (Fig. 5). This observation suggests that using ERT can detect smaller amounts of AT contamination and that relatively more significant contamination levels are necessary to absorb a GPR signal fully.

Aydi et al. (2020) wrote that the ERT technique is routinely used to investigate the contamination plumes from municipal and hazardous waste landfills. In our case, the addition of a sharp boundary obtained via GPR data significantly improved our ability to identify a contamination plume. Thus, it can be stated that a combination of ERT and GPR data is a highly effective tool for the analysis of the geospatial distribution of soil and groundwater pollution plumes caused by ATs. Furthermore, the combination of ERT and GPR methods is effective even in areas with complex geological build-up. This potential of combined GPR and ERT surveys for mapping AT contamination could be highly essential and valuable in cases where the number of monitoring wells is limited or their placing is not optimal.

Drawing the exact area of contamination from ERT or GPR data is, however, ambiguous. Using geophysical methods, we have identified a zone of low ground resistivity, but this could not be related to the distribution of specific pollutants and their concentrations directly and without correlations to direct measurements. Many studies have attempted to correlate soil properties with measured apparent resistivity values (see the review of Friedmann 2005) and the effects of various contaminants on apparent resistivity have been tested (Liu et al. 2008; Gabarrón et al. 2020). However, only a few studies have been carried out where the changes in ground electrical resistivity were directly correlated with the concentration of AT decomposition products (e.g. Naudet et al. 2011, 2014). We treat the observed low-resistivity area as an indicator of the presence of a contamination plume (Fig. 5) that is verified by monitoring well data (Ņelajevs 2019). To outline the precise distributions and concentrations of the contaminants, direct methods should be further applied.

CONCLUSIONS

We have shown that the combination of ERT and GPR data is highly effective for analysing the geospatial distribution of soil and groundwater pollution caused by ATLs in an area with a complex geological cross-section – Inčukalns ATL, Latvia. The data obtained by us indicate that the ERT method can be used as the primary tool for investigating the contamination plumes from ATLs. Simultaneously, an initial assessment and survey of the geological structure can be done using GPR data.

Our results demonstrate that the initially assessed distribution of the contamination via borehole data is too conservative. Contamination is spread further away from the historical site of the ATL; furthermore, its migration path does not follow the flow direction of regional groundwater as has been proposed earlier. Combined ERT, GPR and borehole data indicate that the low-resistivity area corresponds to an AT pollution plume.

Geophysical survey data should be used for further decision-making regarding the management of residual

pollution, including the installation of additional monitoring wells for the direct observations of specific components of pollution substances.

Acknowledgements. This work was supported by the Latvian Science Foundation project grant 'Geophysical data integration and application to soil contamination mapping' No. lzp-2020/2-0171 and by the performance-based funding of the University of Latvia within the 'Climate change and sustainable use of natural resources' project. We thank Jüri Plado and an anonymous reviewer for the valuable comments and corrections that improved the quality of the manuscript. The publication costs of this article were partially covered by the Estonian Academy of Sciences.

REFERENCES

Aleksans, O., Levin, I., Anikejeva, R., Semjonov, I. & Gosk, E. 1993. *Incukalns Waste Pools, Problem or Asset? Service Report*. Copenhagen, DGU Geological Survey of Denmark, 32 pp.

Aleksans, O., Levin, I. & Gosk, E. 1994. *Incukalns Investigation, Completion Report. Service Report Nr. 24.* Copenhagen, DGU Geological Survey of Denmark, 55 pp.

Aydi, A., Mhimdi, A., Hamdi, I., Touaylia, S. & Sdiri, A. 2020. Application of electrical resistivity tomography and hydrochemical analysis for an integrated environmental assessment. *Environmental Nanotechnology, Monitoring & Management*, **14**, 100351.

Berzina, A. & Samushenkov, M. 1977. *Otchet o geologo-gidrogeologicheskikh issledovaniyakh po vyyavleniyu vliyaniya svalki kislogo gudrona na podzemnye vody u naselennogo punkta Inchukalns* [*Report of Geological-Hydrogeological Research of the Environmental Impact of Acid Tar Damp near the Inchukalns Village*]. Riga, Ministry of Geology of USSR, 86 pp. [in Russian].

Chambers, J., Ogilvy, R., Meldrum, P. & Nissen, J. 1999. 3D resistivity imaging of buried oil- and tar-contaminated waste deposits. *European Journal of Environmental and Engineering Geophysics*, **4**, 3–15.

Družina, B. & Perc, A. 2010. Remediation of acid tar lagoon. In *Proceedings of the Annual International Conference on Soils, Sediments, Water and Energy*, Vol. 15, Article 17, pp. 195–209.

Friedmann, S. P. 2005. Soil properties influencing apparent electrical conductivity: a review. *Computers and Electronics in Agriculture*, **46**, 45–70.

Gabarrón, M., Martínez-Pagán, P., Martínez-Segura, M. A., Bueso, M. C., Martínez-Martínez, S., Faz, Á. & Acosta, J. A. 2020. Electrical resistivity tomography as a support tool for physicochemical properties assessment of near-surface waste materials in a mining tailing pond (El Gorguel, SE Spain). *Minerals*, **10**, 559–575.

GeoTomo software. 2017. *User Manual: Rapid 2-D Resistivity & IP Inversion Using the Least-Squares Method*. 147 pp.

Grajczak, P. & McManus, R. W. 1995. Remediation of acid tar sludge at a superfund site. *Superfund Proceedings*, **1**, 243–244.

Gruss, O. 2005. Saureharzaltlasten, Innovative Technologien zur Sanierung und energetischen Verwertung [Acid residues, innovative technologies for clean-up and energy recovery]. *Terratech*, **3**–**4**, 15–18.

Hao, X. 2007. *Acid Tar Lagoons: Assessment and Environmental Interaction*. PhD Thesis, University of Sheffield, 222 pp. [https://etheses.whiterose.ac.uk/12858/1/490318.pdf].

Jiang, Y., Li, Y., Yang, G., Zhou, X., Wu, J. & Shi, X. 2013. The application of high-density resistivity method in organic pollution survey of groundwater and soil. *Procedia Earth and Planetary Science*, **7**, 932–935.

Karuša, S. & Demidko, J. 2018. *Pārskats riska pazemes ūdens objekta A11 "Inčukalna sērskābā gudrona dīķi" robežu noteikšanas metodika un stāvokļa raksturojums* [*Overview of the Boundary Setting Methodology and Characterization of Environmental Impact in the Groundwater Risk Object № A11: Inčukalns's Acid Tar Lagoons*]. Latvian Environment, Geology and Meteorology Centre, Riga, 62 pp. [in Latvian].

Karušs, J. & Bērziņš, D. 2015. Ground-penetrating radar study of the Cenas tīrelis bog, Latvia: Linkage of reflections with peat moisture content. *Bulletin of the Geological Society of Finland*, **87**, 87–98.

Kolmakov, G. A., Zanozina, V. F., Karataev, E. N., Grishin, D. F. & Zorin, A. D. 2006. Thermal cracking of acid tars to asphalts as a process for utilisation of refinery wastes. *Petroleum Chemistry*, **46**, 384–388.

Kruglik, S. I. 1990. *Otchet o rezul´tatakh kompleksnykh issledovanij po izucheniyu masshtabov zagryazneniya gruntovykh vod v rajone raspolozheniya svalok sernokislogo gudrona v rajone nas. p. Inchukalns* [*Report of the Complex Research of Groundwater Pollution near the Acid Tar Lagoons in the Vicinity of Inchukalns Village*]. Company Vodgeo, 80 pp. [in Russian].

Lamsters, K., Karušs, J., Stūrmane, A., Ješkins, J. & Džeriņš, P. 2020. Mapping of large-scale diapir structures at the paleo-ice tongue bed in western Latvia from geophysical investigations and borehole data. *Quaternary International*, DOI: 10.1016/j.quaint.2020.12.003.

Leonard, S. A., Stegemann, J. A. & Roy, A. 2010. Characterisation of acid tars. *Journal of Hazardous Materials*, **175**(1–3), 382–392.

Liu, S., Chen, L. & Han, L. 2008. Study on electrical resistivity related parameters of contaminated soils. In *Geotechnical Engineering for Disaster Mitigation and Rehabilitation* (Liu, H. & Chu, J., eds), pp. 695–701. Beijing.

Loke, M. H. 2004. *Tutorial: 2-D and 3-D Electrical Imaging Surveys. Geotomo Software, Res2dinv 3.5 Software*, 136 pp.

Loke, M. H. & Barker, R. D. 1996. Rapid least-squares inversion of apparent resistivity pseudosections using a quasi-Newton method. *Geophysical Prospecting*, **44**, 131–152.

Milne, D. D., Clark, A. I. & Perry, R. 1986. Acid tars: their production, treatment and disposal in the UK. *Waste Management & Research*, **4**, 407–418.

Nancarrow, D. J., Slade, N. J. & Steeds, J. E. 2001. *Land Contamination: Technical Guidance on Special Sites: Acid Tar Lagoons*. R & D Technical Report P5-042/TR/04. Environment Agency, 62 pp.

Naudet, V., Gourry, J. C., Mathieu, F., Girard, J. F., Blondel, A. & Saada, A. 2011. 3D electrical resistivity tomography to locate DNAPL contamination in an urban environment. In *Conference Proceedings, Near Surface 2011-17th EAGE European Meeting of Environmental and Engineering*

Geophysics. European Association of Geoscientists & Engineers, cp-253-00021.

Naudet, V., Gourry, J. C., Girard, F., Mathieu, F. & Saada, A. 2014. 3D electrical resistivity tomography to locate DNAPL contamination around a housing estate. *Near Surface Geophysics*, **12**, 351–360.

Neal, A. 2004. Ground-penetrating radar and its use in sedimentology: principles, problems and progress. *Earth-Science Reviews*, **66**, 261–330.

Ņelajevs, A. 2019. *Vides monitorings objektā "Vēsturiski piesārņota vieta "Inčukalna sērskābā gudrona dīķi"". 2019. gada I pusgads (Monitoringa darbu programmas III cikls). Atskaites ziņojums* [*Environmental Monitoring at the Object "Historically Polluted Place "Inčukalns Acid Tar Lagoon"". First Half of 2019 (Monitoring Work Program cycle III) Report*]. Azurits Ltd, 154 pp. [in Latvian].

Pensaert, S. 2005. The remediation of the acid tar lagoons, Rieme, Belgium. In *Stabilisation/Solidification Treatment and Remediation: Proceedings of the International Conference on Stabilisation/Solidification Treatment and Remediation, 12–13 April 2005, Cambridge, UK*, pp. 255–259. CRC Press.

Power, C., Gerhard, J. I., Tsourlos, P., Soupios, P., Simyrdanis, K. & Karaoulis, M. 2015. Improved time-lapse electrical resistivity tomography monitoring of dense non-aqueous phase liquids with surface-to-horizontal borehole arrays. *Journal of Applied Geophysics*, **112**, 1–13.

Reynolds, J. M. 1997. *An Introduction to Applied and Environmental Geophysics*. Wiley, New York, 806 pp.

Reynolds, J. M. 2002. The role of environmental geophysics in the investigation of an acid tar lagoon, Llwyneinion, North Wales, UK. *First Break*, **20**, 630–636.

Smith, C., Hao, X., Talbot, S. & Lawson, N. 2008. *Acid Tar Lagoons.* https://www.claire.co.uk/component/phocadownload/file/34-Other-CLAIRE-Documents?Itemid=230 [accessed 20 February 2021].

State Environmental Agency. 2020. *Valsts vides dienests iepazīstina Inčukalna novada iedzīvotājus ar aktualitātēm sērskābā gudrona dīķu sanācijā* [*State Environmental Agency Communicates Current Events Related to the Clean-Up of Inchukalns's Acid Tar Lagoons with Local Inhabitants*]. http://www.vvd.gov.lv/jaunumi/2020/07/valsts-vides-dienests-iepazistina-incukalna-novada-iedzivotajus-ar-akt?id=1196 [in Latvian; accessed 20 February 2021].

Läti Inčukalnsi happetõrvabasseini jääkreostuse geofüüsikaline kaardistamine

Janis Karušs, Kristaps Lamsters, Dmitrijs Poršņovs, Viesturs Zandersons ja Jurijs Ješkins

Happetõrvabasseinid on tööstusriikides laialt levinud keskkonnaprobleemiks kogu maailmas. Nendest on saanud olulised ja ulatuslikud keskkonnareostuse allikad, mis mõjutavad mulda, atmosfääri ning pinna- ja põhjavett. Artiklis on uuritud pinnase ja põhjavee jääkreostust Lätis Lõuna-Inčukalnsi happetõrvabasseini ümbruses, kasutades kombineeritult georadarit ning elektromeetrilist meetodit. Saadud andmed iseloomustavad uuringuala geoloogilisi struktuure ja näitavad saasteainete levikut. Töös on piiritletud madala elektritakistusega tsooni paiknemine pinnases ja seostatud seda jääkreostuse levikuga. Uuring näitab, et georadari ja elektromeetria kombinatsioon on tõhus vahend happetõrvabasseinide põhjustatud pinnase- ning põhjaveereostuse leviku analüüsimisel kompleksse geoloogilise ehitusega aladel.